

SANDIA REPORT

SAND2013-1603

Unlimited Release

Printed February 2013

PV Output Smoothing using a Battery and Natural Gas Engine-Generator

Jay Johnson, Abraham Ellis, Atsushi Denda, Kimio Morino, Takao Shinji, Takao Ogata, and Masayuki Tadokoro

Prepared by
Sandia National Laboratories
Albuquerque, New Mexico 87185 and Livermore, California 94550

Sandia National Laboratories is a multi-program laboratory managed and operated by Sandia Corporation, a wholly owned subsidiary of Lockheed Martin Corporation, for the U.S. Department of Energy's National Nuclear Security Administration under contract DE-AC04-94AL85000.

Approved for public release; further dissemination unlimited.



Sandia National Laboratories

Issued by Sandia National Laboratories, operated for the United States Department of Energy by Sandia Corporation.

NOTICE: This report was prepared as an account of work sponsored by an agency of the United States Government. Neither the United States Government, nor any agency thereof, nor any of their employees, nor any of their contractors, subcontractors, or their employees, make any warranty, express or implied, or assume any legal liability or responsibility for the accuracy, completeness, or usefulness of any information, apparatus, product, or process disclosed, or represent that its use would not infringe privately owned rights. Reference herein to any specific commercial product, process, or service by trade name, trademark, manufacturer, or otherwise, does not necessarily constitute or imply its endorsement, recommendation, or favoring by the United States Government, any agency thereof, or any of their contractors or subcontractors. The views and opinions expressed herein do not necessarily state or reflect those of the United States Government, any agency thereof, or any of their contractors.

Printed in the United States of America. This report has been reproduced directly from the best available copy.

Available to DOE and DOE contractors from

U.S. Department of Energy
Office of Scientific and Technical Information
P.O. Box 62
Oak Ridge, TN 37831

Telephone: (865) 576-8401
Facsimile: (865) 576-5728
E-Mail: reports@adonis.osti.gov
Online ordering: <http://www.osti.gov/bridge>

Available to the public from

U.S. Department of Commerce
National Technical Information Service
5285 Port Royal Rd.
Springfield, VA 22161

Telephone: (800) 553-6847
Facsimile: (703) 605-6900
E-Mail: orders@ntis.fedworld.gov
Online order: <http://www.ntis.gov/help/ordermethods.asp?loc=7-4-0#online>



SAND2013-1603
Unlimited Release
Printed February 2013

PV Output Smoothing using a Battery and Natural Gas Engine-Generator

Jay Johnson and Abraham Ellis
Sandia National Laboratories
P.O. Box 5800
Albuquerque, New Mexico 87185-0352

Atsushi Denda and Kimio Morino
Shimizu Corporation

Takao Shinji, Takao Ogata, and Masayuki Tadokoro
Tokyo Gas Co., Ltd.

Abstract

In some situations involving weak grids or high penetration scenarios, the variability of photovoltaic systems can affect the local electrical grid. In order to mitigate destabilizing effects of power fluctuations, an energy storage device or other controllable generation or load can be used. This paper describes the development of a controller for coordinated operation of a small gas engine-generator set (genset) and a battery for smoothing PV plant output. There are a number of benefits derived from using a traditional generation resource in combination with the battery; the variability of the photovoltaic system can be reduced to a specific level with a smaller battery and Power Conditioning System (PCS) and the lifetime of the battery can be extended. The controller was designed specifically for a PV/energy storage project (Prosperity) and a gas engine-generator (Mesa Del Sol) currently operating on the same feeder in Albuquerque, New Mexico. A number of smoothing simulations of the Prosperity PV were conducted using power data collected from the site. By adjusting the control parameters, tradeoffs between battery use and ramp rates could be tuned. A cost function was created to optimize the control in order to balance, in this example, the need to have low ramp rates with reducing battery size and operation. Simulations were performed for cases with only a genset or battery, and with and without coordinated control between the genset and battery, e.g., without the communication link between sites or during a communication failure. The degree of smoothing without coordinated control did not change significantly because the battery dominated the smoothing response. It is anticipated that this work will be followed by a field demonstration in the near future.

ACKNOWLEDGMENTS

This work was funded by the U.S. Department of Energy Solar Energy Technologies Program and Office of Electricity Energy Storage Program. We also acknowledge the contribution of Public Service Company of New Mexico (PNM), as well as Japan's New Energy and Industrial Development Organization (NEDO), Shimizu and Tokyo Gas for providing access to critical data.

CONTENTS

CONTENTS	5
FIGURES	6
TABLES.....	6
NOMENCLATURE.....	7
1. INTRODUCTION.....	9
2. Smoothing Control Algorithm Design	10
2.1 Combined Gas Engine-Generator and Battery Controller	10
2.2 Gas Engine-Generator Characteristics.....	13
3. Gas Engine-Generator and Battery Simulations	13
3.1 Influence of the Control Parameters	16
3.1.1 Influence of GE_{gain}	17
3.1.2 Influence of T_w	18
3.1.3 Influence of K_{SOC}	19
3.1.4 Influence of K_{GE}	19
3.1.5 Influence of GE Delay	20
3.2 Figures of Merit	21
3.2 Control Optimization	22
4. Alternative Control Schemes	27
4.1 Controlling ramp rates with only the battery or gas engine-generator	27
4.2 Simulations without GE-Battery Coordinated Control.....	29
5. CONCLUSIONS.....	33
REFERENCES.....	34
DISTRIBUTION.....	36

FIGURES

Figure 1. Mesa del Sol distribution system.....	9
Figure 2. Control scheme for the battery and gas engine-generator.....	12
Figure 3. Gas engine-generator response to step changes in power reference.....	13
Figure 4. The influence of the gas engine-generator on battery operation.....	14
Figure 5. Detail of Figure 4, showing power production from the battery and gas engine-generator.....	15
Figure 6. Cumulative distribution function of the 1-minute power ramp rates for the P_{PV} , $P_{PV}+P_{bat}$, and $P_{PV}+P_{bat}+P_{GE}$	16
Figure 6. GE_{gain} effect on battery and gas engine-generator operation.....	17
Figure 7. T_w effect on battery and gas engine-generator operation.....	18
Figure 8. K_{SOC} effect on battery and gas engine-generator operation.....	19
Figure 9. K_{GE} effect on battery and gas engine-generator operation.....	20
Figure 10. Influence of GE Delay on gas engine-generator operation.....	21
Figure 11. Power profiles for the LHS simulations.....	22
Figure 12. Latin Hypercube Sampling results for Day 1.....	24
Figure 13. Latin Hypercube results for all 5 days.....	25
Figure 14. Influence of control parameters on FOMs and total fitness.....	27
Figure 15. Three-dimensional representation of the fitness profile.....	27
Figure 16. Power production when the GE or battery are unavailable.....	28
Figure 17. Ramp rate CDFs for Day 1 when the GE or battery are unavailable.....	29
Figure 18. Control scheme for the battery and gas engine-generator without communication from the gas engine-generator to the battery.....	30
Figure 19. PV smoothing with and without communication from the GE to battery.....	31
Figure 20: Difference in FOMs depending on communication from the GE to the Battery. Blue is with coordinated control.....	32

TABLES

Table 1: Summary of MATLAB/Simulink parameters for battery + GE controllers.....	17
--	----

NOMENCLATURE

AC	alternating current
AvgGEPower	average gas engine-generator power production
BatSOCRange	battery state of charge range
BatWork	work done by the battery
CDF	cumulative distribution function
DC	direct current
GE	gas engine-generator
GE Delay	gas engine-generator control signal delay
GE _{gain}	proportional gain to adjust gas engine-generator use
GEwear	gas engine-generator wear, defined by the change in power
Hz	hertz
K _{GE}	gas engine-generator proportional control to return the GE to the nominal power
K _{SOC}	battery proportional control to return the battery to the reference SOC
kW	kilowatt
kWh	kilowatt-hour
LHS	latin hypercube sampling
MaxBatkW	maximum instantaneous output power of the battery
MdS	Mesa del Sol
MPP	maximum power point
MW	megawatt
NEDO	New Energy and Industrial Development Organization of Japan
PCC	point of common coupling (grid interconnect)
PCS	battery power conditioning system
P _{bat}	battery power output
P _{bat-SP}	battery power setpoint sent to battery
P _{error}	difference in power between the PV and moving average
P _{GE}	gas engine-generator power output deviation from nominal output
P _{GE-SP}	gas engine-generator controller setpoint sent to genset
P _{smooth}	the smooth power (calculated by the moving average of P _{PV})
P _{PV}	photovoltaic power
PNM	Public Service Company of New Mexico
PV	photovoltaic
RMS	root-mean-square

RR ₉₉	1-minute ramp rate at the 99th percentile of the ramp rate CDF.
SNL	Sandia National Laboratories
SOC	state of charge
SOC _{max}	maximum state of charge of the battery
SOC _{min}	minimum state of charge of the battery
SOC _{ref}	reference state of charge ($1/2*(SOC_{max} + SOC_{min})$)
SQP	sequential quadratic programming
T _w	window of time for the controller moving average
UNM	University of New Mexico

1. INTRODUCTION

In some cases involving weak grids or high penetration scenarios, local storage systems are introduced to mitigate adverse impacts due to variability of renewable generation on the electrical grid. These storage systems (e.g. batteries) smooth the renewable power output so that the local grid voltage (and frequency in the case of island grids) is not negatively impacted. As part of a DOE-sponsored energy storage demonstration, Public Service Company of New Mexico (PNM) has a 500 kW photovoltaic (PV) system co-located with a 500 kW, 330 kWh valve-regulated lead-acid (VRLA) smoothing battery [1] at the Prosperity site near the Albuquerque Airport. The battery is currently used to demonstrate smoothing of the PV power, using a control algorithm developed by Sandia [2]. The New Energy and Industrial Development Organization of Japan (NEDO), in partnership with PNM, the University of New Mexico, and Sandia National Labs has developed a smart grid demonstration project at Mesa del Sol, to investigate, among other things, the benefits of using traditional generation in addition to storage to control PV power variability [3]. The Prosperity and Mesa del Sol projects are installed on the same 12.47 kV feeder (PNM Studio 14). This report describes optimized operation of the gas engine-generator (genset) and the battery, with respect to factors such as the size of the battery, size of the battery inverter, and the lifetime of the battery. The Mesa del Sol and Prosperity projects are shown in Figure 1. The smoothing control was designed for the 500 kW power battery.

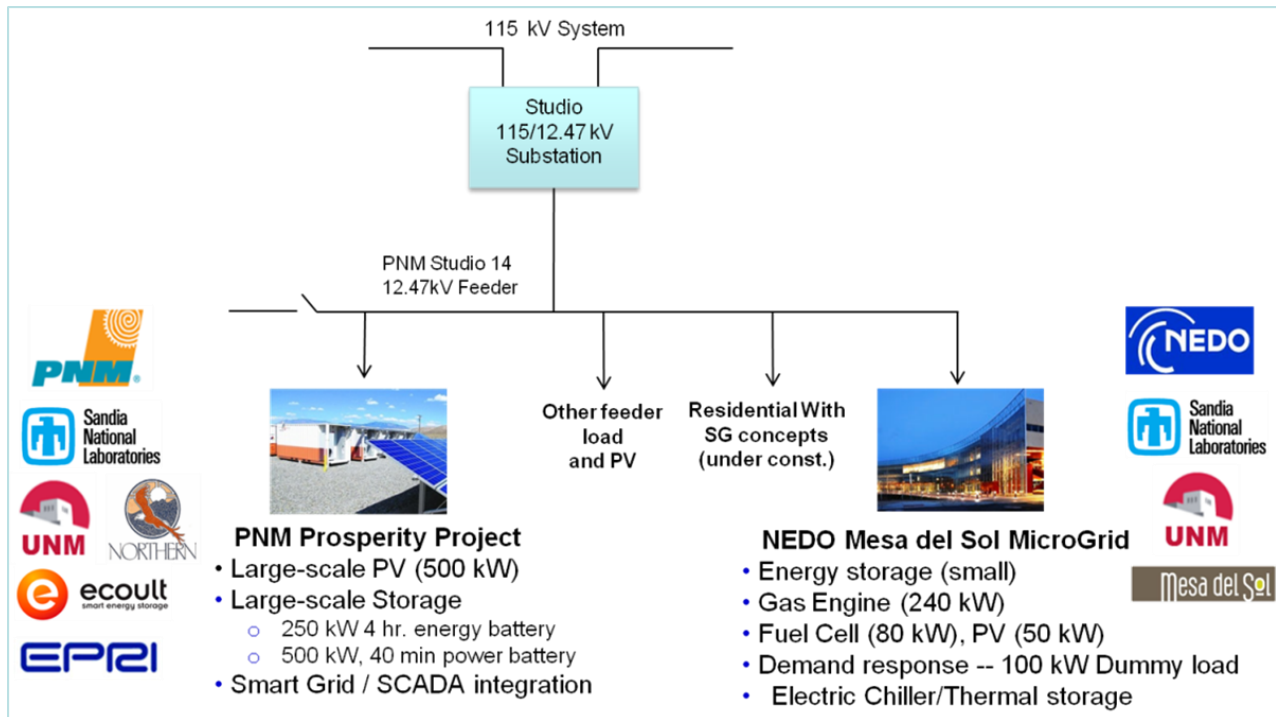


Figure 1. Mesa del Sol distribution system.

The control algorithm currently employed by the battery system was an area of previous study [2]. This controller was modified to include the addition of the gas engine-generator. In the extended, coordinated control formulation, the gas genset receives the near real-time power

signal from the Prosperity site and adjusts its power in conjunction with the battery to smooth the PV power output.

2. Smoothing Control Algorithm Design

The use of battery to reduce the variability of PV and wind generation systems has been the subject of much research [3-7]. Recently, a few commercial PV and wind projects have been installed in Hawaii with co-located energy storage to meet specific output variability limits at the point of common coupling (PCC) [8]. Other island jurisdictions are considering similar output variability limits that could drive need for energy storage or other mitigation alternative [9]. It should be noted that these requirements for ramp rate limits at the PCC are only applicable to specific circumstances where the variable generation project can cause local voltage or system frequency impacts. For larger interconnected grids, and even island grids, a more cost-effective use of energy storage systems would be to help maintain grid stability by supporting system voltage and frequency [10-12]. In the case of the Prosperity project, the PV system was co-located with a battery as a demonstration, to learn how a utility could manage distributed resources to contribute to various grid support objectives, including variability reduction or smoothing.

2.1 Combined Gas Engine-Generator and Battery Controller

The existing PNM battery-PV smoothing control [2] determines the desired power required from a controllable resource (battery or gas engine-generator) using a moving average sliding window or low-pass-filtered version of the PV power history. The idea is that the controllable resource would make up the difference between the PV power output and the smoothed power output profile (i.e., error signal). The difference between this implementation and the extended work described in this document is that both the battery and the gas engine-generator, as opposed to just the battery, respond to the error signal. The gas engine-generator is significantly slower than the PV and the battery, so it is only able to completely relieve the battery from operating during slow ramp rates. The faster ramp rates are still nearly fully tasked to the battery. After accounting for limitations such as engine-generator rating and battery state of charge (SOC) limits, the overall smoothing control formulation has several degrees of freedom. This means that control parameters can be optimized based on other factors like operational cost and battery lifetime. In the same manner, simulation-based optimization can be used to determine the required size of energy storage capacity and associated power conditioning system (PCS).

The 240 kW gas engine-generator requires a minimum output of 120 kW to operate with a reasonable efficiency and emissions levels. Accordingly, it is assumed that the gas engine-generator operates between 120 kW and 240 kW. When in operation, the gas engine-generator output has a return signal to adjust the output to a nominal value at the center of the operating range (e.g., 180 kW) so that it can respond in the positive and negative directions by reducing or increasing power output. For the purposes of smoothing, contribution of the gas engine-generator, P_{GE} , is defined as the power change from nominal, such that $-60 \text{ kW} < P_{GE} < 60 \text{ kW}$. In the actual implementation at Mesa del Sol, the genset power limits are enforced by a separate genset controller. Similarly, the controller should return the energy storage SOC to a nominal

value near the center of the SOC range, at a rate that is slow compared to the energy storage ramping capability. For example, the SOC limits (SOC_{min} and SOC_{max}) may be 20% and 80%, respectively, and the reference SOC (SOC_{ref}) may be 50%¹. These SOC levels will vary on the application, battery technology, and smoothing controller design. In the actual implementation at Prosperity, the SOC limits are enforced by a separate battery energy system controller.

In summary, the real-time controller performs the following actions:

1. Determines the desired, smooth power of the system, P_{smooth} , using a moving average or low pass filter based on the time history of PV power, P_{PV} .
2. Issues power reference commands to the energy storage system and engine control to ensure the total power from the generators is *nearly* equal to the smoothed power profile: $P_{smooth} \cong P_{pv} + P_{bat} + P_{GE}$, where P_{bat} is the battery power and P_{GE} is defined as the GE power change from nominal, as described above.
3. Slowly, return the battery SOC and genset output to a nominal level, as described above.

The PV power error is defined by the difference in P_{smooth} and P_{PV} and will be approximately the power generated by the gas engine-generator and the battery,

$$P_{error} = (P_{smooth} - P_{pv}) \cong P_{GE} + P_{bat} \quad (1)$$

In an actual implementation, P_{error} cannot be expected to be zero at all times because of communication and processing delays, and limits imposed by the battery and genset controllers.

The controller is shown in Figure 2. As shown in the upper grey block of Figure 2, PV error signal (smoothing requirement) is calculated by the battery smoothing control, which is co-located with the PV and energy storage system. This error signal is transmitted to the gas engine-generator control. The output of the gas engine-generator control is subtracted from the error signal and transmitted to the battery smoothing control to compute the battery set point. This control architecture is suitable for the smoothing application because the gas engine-generator is much slower than the battery, so the battery can make up for the power that the GE is unable to produce. Further, battery life is more sensitive to power production than the GE, so this hierarchical structure helps extend the lifetime of the battery.

The gas engine-generator and battery controllers are similar. The error signal first is passed through a dead band which forces the error to reach a certain point before the controller responds. The dead band is set to zero for all simulations in this report. There is a gain that scales the error signal reaching the genset and battery. The scaling factor for the genset, GE_{gain} , varies in the simulations and the battery controller gain is set to unity (and therefore not shown in Figure 2). A scaling factor of unity for the energy storage smoothing control is reasonable for this particular project, given that the rating of the PV inverter the energy storage PCS are both 500 kW. The control signal is returned to P_{GE_nom} and SOC_{ref} for the GE and battery using a proportional gain feedback control. The values of K_{GE} and K_{SOC} are small relative to the ramping capability of the genset and battery to ensure that smoothing control has priority, but over time return the GE to P_{GE_nom} and the battery to SOC_{ref} . The resulting genset and battery

¹ SOC percentages are with respect to battery capacity.

power setpoints are sent to the gas engine-generator and battery plants. In the simulations discussed in this paper, the energy storage is represented as a simple integrator, which ignores battery losses. Battery storage hardware-driven ramp limits are higher than requirements placed on the battery, so the limits are not represented in the simulations or in the model of the battery plant in Figure 2. For the simulations discussed in this paper, $SOC_{min} = 20\%$, $SOC_{max} = 80\%$, and $SOC_{ref} = 50\%$. In an actual application, SOC limits may be selected based on the battery technology and lifetime predictions. For the purposes of the simulations discussed in this paper, the gas engine-generator is represented with a simple rate limit of 0.285 kW/second. This was based on performance tests (see Section 2.2). The genset operational limits are related to the engine performance and emissions considerations. Finally these control signals experience a communication delay before adjusting the power at the plant.

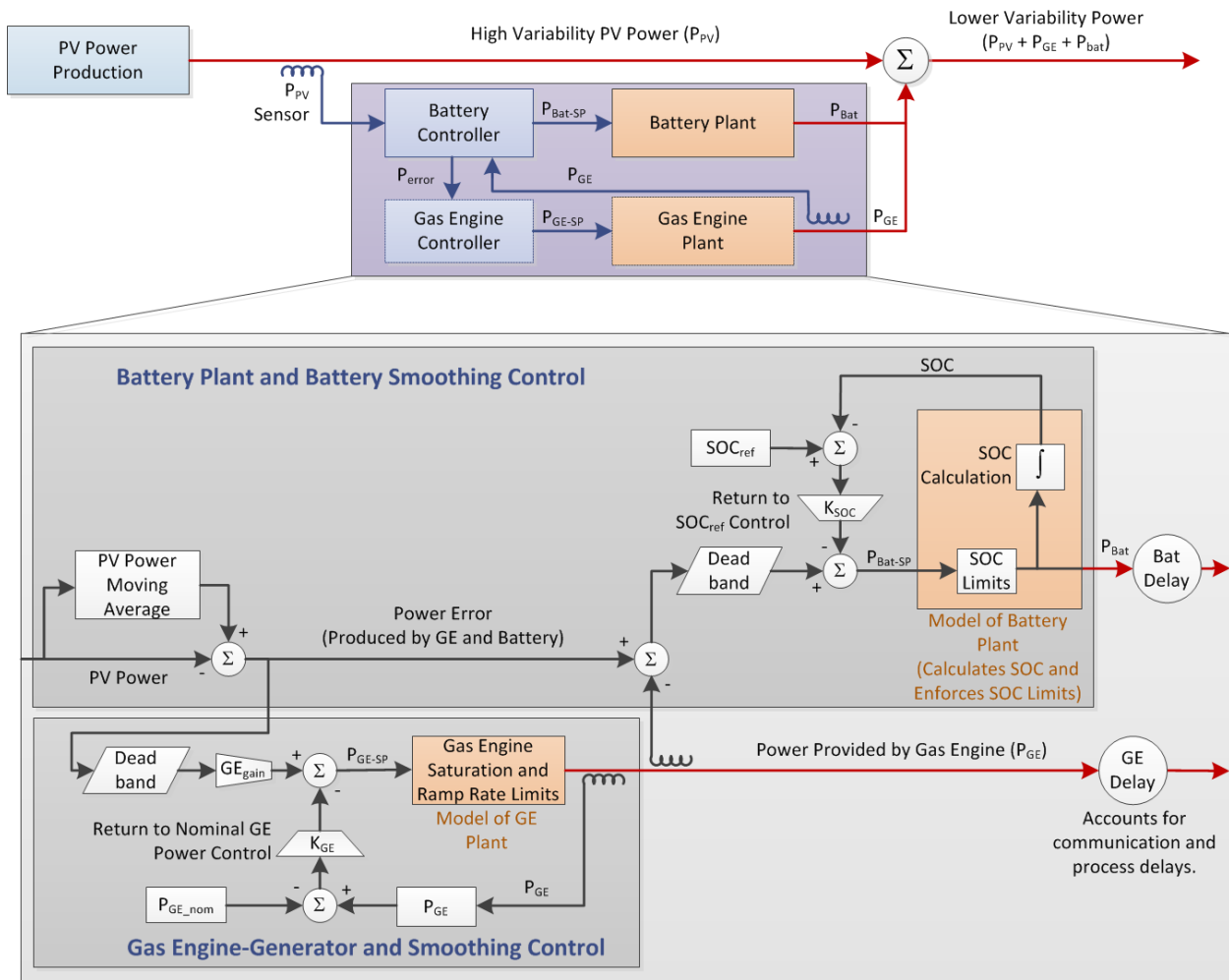


Figure 2. Control scheme for the battery and gas engine-generator.

2.2 Gas Engine-Generator Characteristics

Knowledge of the gas engine-generator ramping capability in the operating range of the GE (120-240 kW) was required in order to simulate the power production of the genset. The response of the genset to downward and upward step changes in reference power were measured, as shown in Figure 3. The response is nearly linear, with little variation in ramp rate. For simplicity, the average rate of ± 0.285 kW/s was used in the simulations.

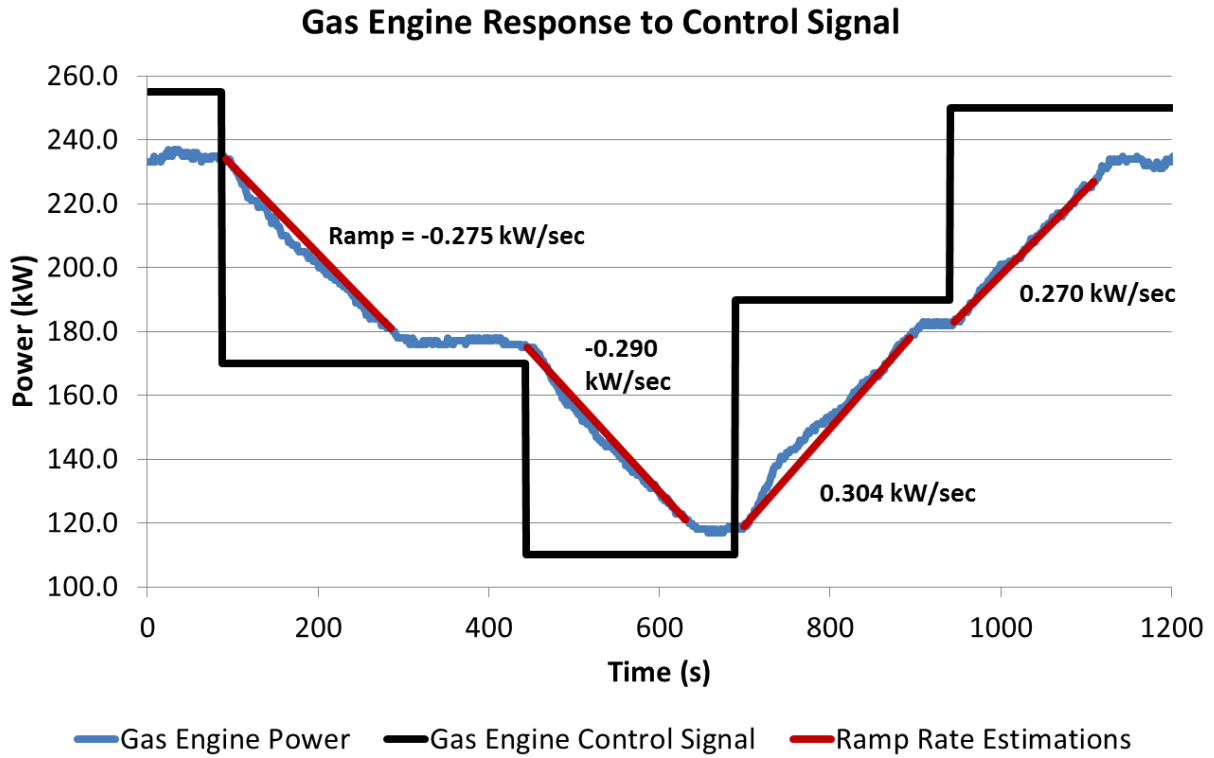


Figure 3. Gas engine-generator response to step changes in power reference.

3. Gas Engine-Generator and Battery Simulations

Prosperity PV output data from five different days was used to simulate smoothing using the gas engine-generator and battery. These simulations were used to identify appropriate ranges for control parameters to optimize the smoothing control. A simulation of one of the daily output profiles shown in Figure 4 shows that the genset is not fast enough to keep up with the larger ramp rates and often saturates, but it does significantly reduce the SOC range the battery, shown in the bottom plot. The PV output is depicted at the top image along with the smoothed profile. The middle image shows the battery operation with and without the help of the gas engine-generator. In this simulation, the control parameters were set to the default values shown in Table 1.

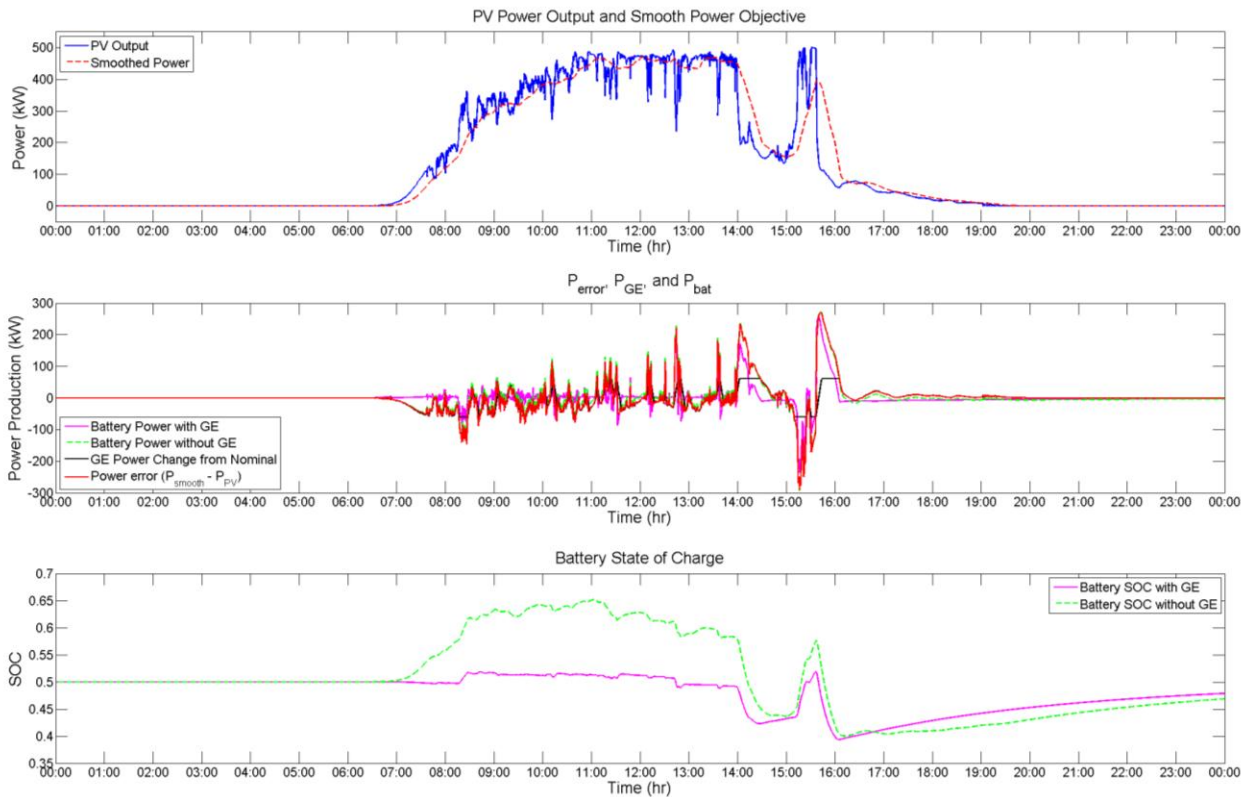


Figure 4. The influence of the gas engine-generator on battery operation.

The inability for the gas engine-generator to reduce the magnitude of fast PV output ramps can be clearly seen by examining the period after 2 PM, when there is a large ramp in the PV output due to a cloud shadow passing over the PV array. As shown in Figure 5, even though the slow gas engine-generator cannot respond quick enough or with enough power to significantly counteract the P_{error} signal, the power output requirements of the battery are reduced by the gas engine-generator response. In this case, the SOC range of the battery is reduced from 25.1% to 12.6% and the maximum PCS instantaneous power requirement is reduced from 292.6 to 260.4 kW. In a design situation, this means that the required size of the battery, the storage capacity of the battery, and the battery PCS can be reduced if a secondary generator such as a genset is available to assist with smoothing. Furthermore, in the case of smaller P_{error} ramps, as shown after 2:30 PM in Figure 5, the gas engine-generator can, at times, fully smooth the PV output and the battery does not have to be employed at all.

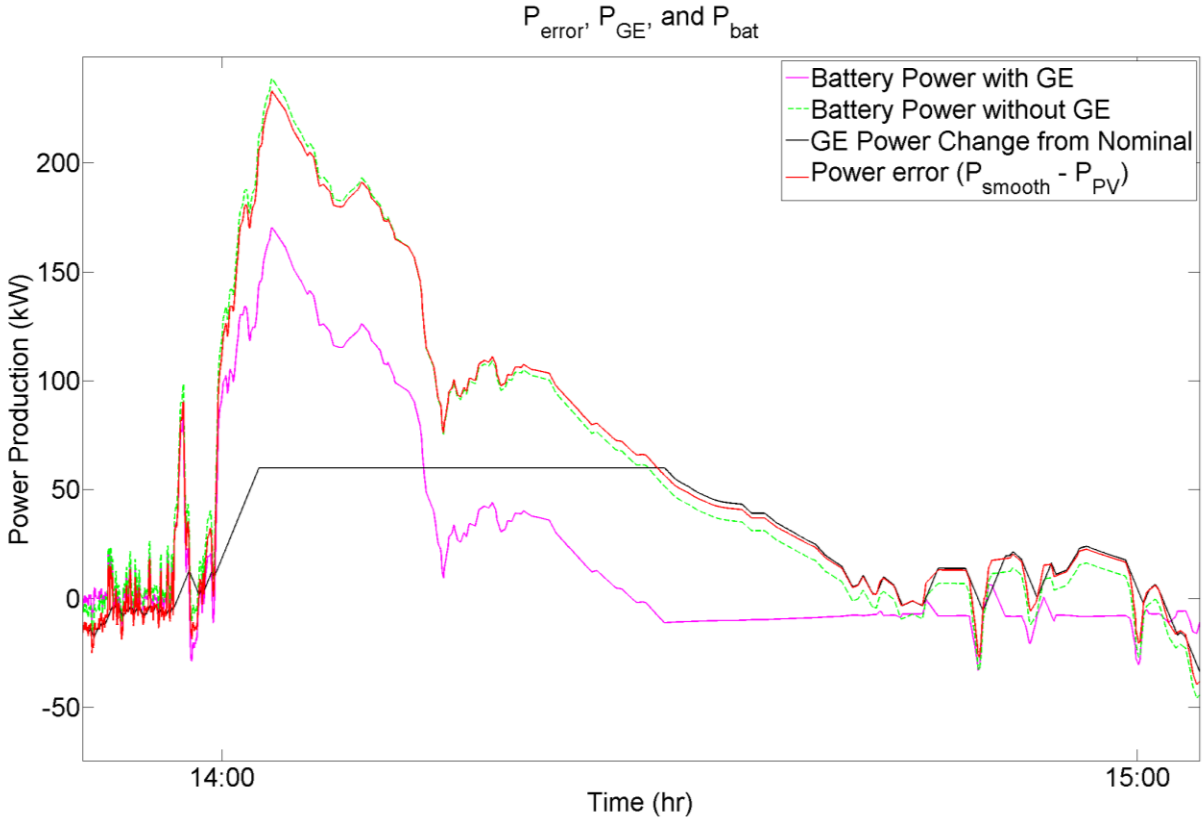


Figure 5. Detail of Figure 4, showing power production from the battery and gas engine-generator.

Figure 6 depicts a cumulative distribution function (CDF) of the 1-minute PV output ramps and the smoothing effect of the battery on PV output. Note that the reduction in variability needs to be defined in terms of a specific statistical term. A simple way is to compare the maximum ramps, however, this metric is subject to measurement noise and fault events (such as inverter trips). As a result, in this paper, a high percentile (i.e., the 99th percentile) of ramps is used as the smoothing metric. Additional discussion of ramp rates is provided in [13].

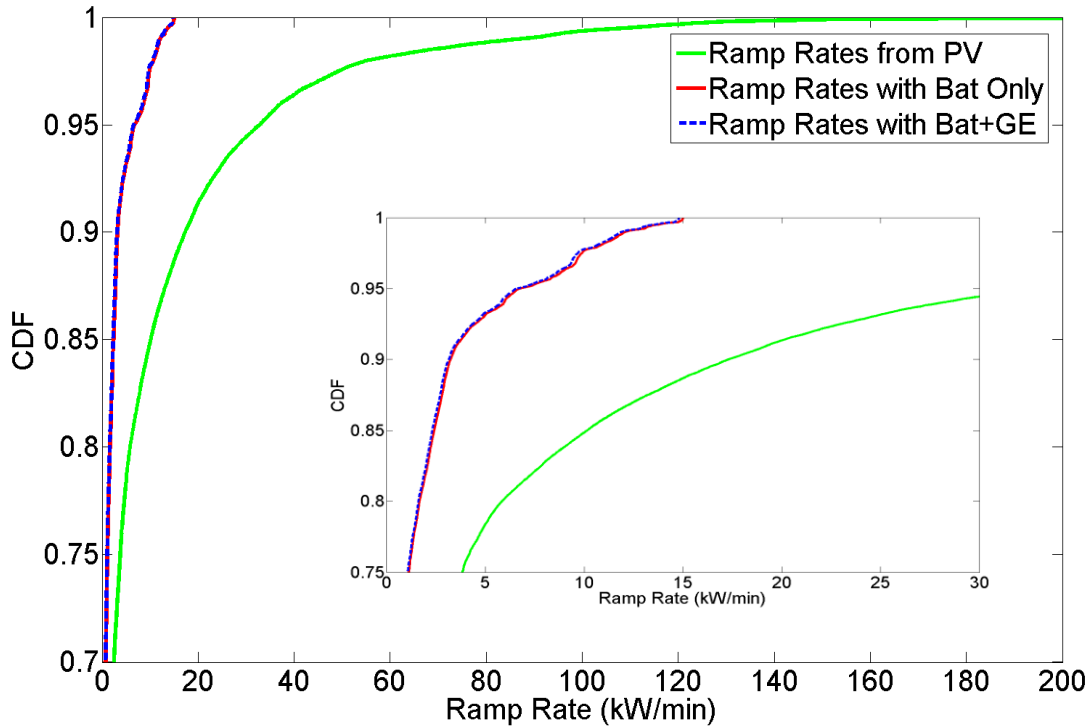


Figure 6. Cumulative distribution function of the 1-minute power ramp rates for the P_{PV} , $P_{PV}+P_{bat}$, and $P_{PV}+P_{bat}+P_{GE}$.

3.1 Influence of the Control Parameters

The simulations above indicate that traditional power generation such as a genset can be operated to supplement a battery to perform smoothing using a simple controller. However, the optimal control for this application has not been investigated. There were a number of parameters in the controller that could be adjusted to improve the performance of the controller. The parameters included in this study were:

1. GE_{gain} – The amount of power error that the gas engine-generator attempts to eliminate.
2. T_w – The window of time that the moving average uses to calculate P_{smooth} .
3. K_{SOC} – The proportional controller used to return the battery to SOC_{ref} .
4. K_{GE} – The proportional controller used to return the GE to the nominal GE power. This is selected to be a percentage of the maximum ramp rate of the GE, $GE_{RRSat} = 0.285$ kW/s, so the smoothing control has priority over the GE return signal.
5. GE Delay – Amount of time that the GE takes to respond to a change in power setpoint, P_{GE-SP} .

The parameter values selected for these studies are shown in Table 1.

Table 1: Summary of MATLAB/Simulink parameters for battery + GE controllers.

Parameter	Default Value	Range of Values
GE_{gain}	1	0-1
T_w	300 s	300-1800 s
K_{SOC}	100	10-1000
K_{GE}	$0.2 \cdot GE_{RRSat}$	$0.05 \cdot GE_{RRSat} - 0.5 \cdot GE_{RRSat}$
GE Delay	0 s	0-5 s

3.1.1 Influence of GE_{gain}

GE_{gain} is the gain on the P_{error} signal entering the gas engine-generator controller. In general, a value of GE_{gain} can be selected based on the relative size of the distributed resource. For the particular conditions of the Prosperity project, this value ranges between 0 and 1. $GE_{gain} = 1$ means that the genset will be more responsive to P_{error} and the battery will be working the least. $GE_{gain} = 0$ means that the GE does nothing to compensate for PV power changes. The battery will have to work the hardest in this case. A demonstration of this gain on the gas engine-generator and battery control is shown in Figure 7. Notice that at $GE_{gain} = 0$, the GE does not deviate from the nominal power of 180 kW and the battery closely matches the P_{error} signal. When GE_{gain} is increased, the gas engine-generator attempts to absorb more of the error signal until it reaches the saturation point (+60 kW). The difference in P_{error} and P_{GE} where the arrow is pointing is the result of the “return to nominal” signal in the controller. Note the P_{error} signal is not affected by GE_{gain} because it is only a function of the PV power.

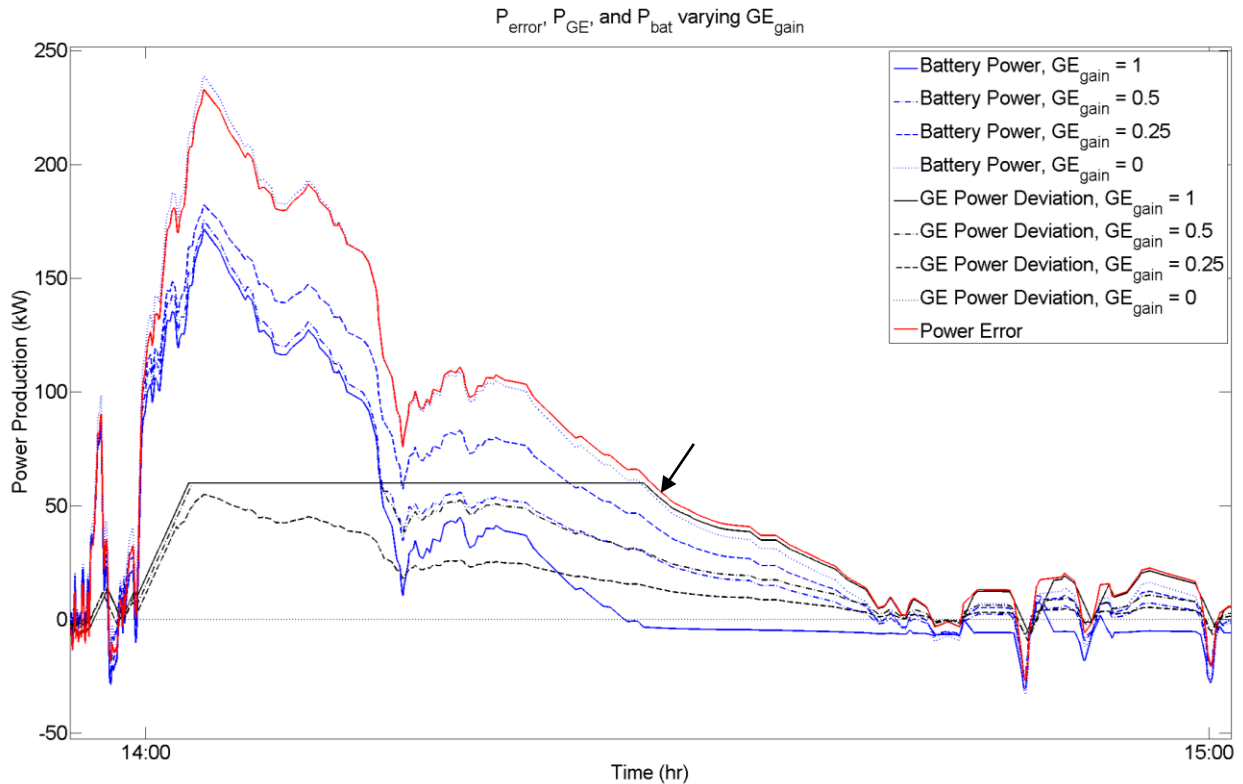


Figure 7. GE_{gain} effect on battery and gas engine-generator operation.

3.1.2 Influence of T_w

T_w is the time window for the sliding average. In the previous simulations, a moving average of 5 minutes (300 s) was used, but this value can be adjusted to change the aggressiveness of the smoothing, which impacts the ramp rates and energy use of the GE and battery. With longer sliding windows, the degree of smoothing is greater, so P_{error} is large, and therefore the battery and gas engine-generator work much harder. When T_w is smaller, the output is less smooth, and P_{error} is smaller so the battery and GE do not work as hard. As shown in Figure 8, the GE often saturates with the large T_w values which means the battery is also forced to work harder. One metric for battery cycle life expectation is total amp-hour throughput [14]. With the smaller T_w values, the battery response is less (closer to 0 kW), so a longer battery life would be expected. However, the degree of smoothing will be smaller in that case, so there are trade-offs to be considered.

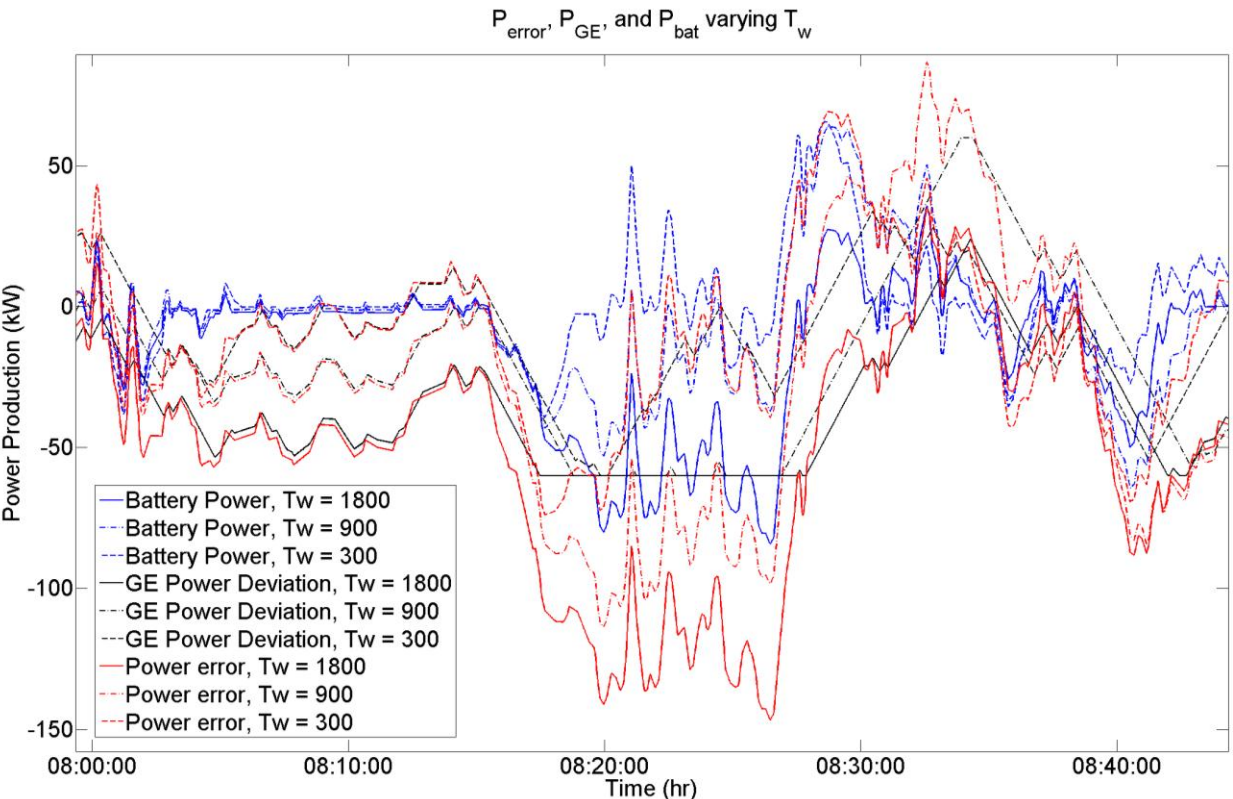


Figure 8. T_w effect on battery and gas engine-generator operation.

3.1.3 Influence of K_{SOC}

Larger K_{SOC} values return the battery to SOC_{ref} more quickly. This means that there is more control error (i.e. P_{error} is not matched by $P_{bat} + P_{GE}$), but the battery is less likely to reach the SOC_{min} or SOC_{max} limits. As shown in Figure 9, the control architecture is such that the battery output has no influence on the operation of the genset. In the case of strong SOC reset control ($K_{SOC} = 1000$), the battery returns more forcibly to the reference SOC level. This affect is seen from 2:30 PM to 3:00 PM when the $K_{SOC} = 1000$ control is significantly far from $P_{bat} = 0$ (meaning the control is working very hard to drive the battery back to SOC_{ref}). Unfortunately, this means when the battery is far from SOC_{ref} , P_{bat} will be farther from $P_{error} - P_{GE}$, and will lead to slightly higher power ramps.

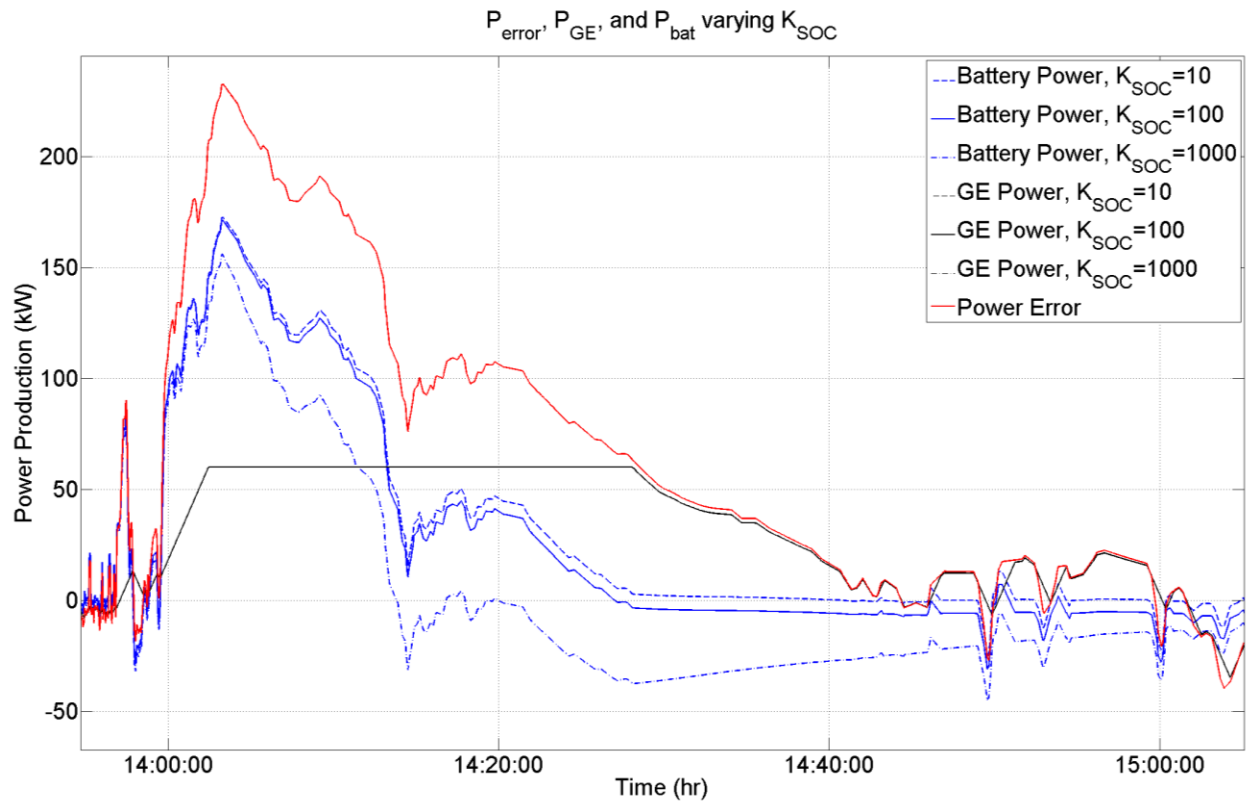


Figure 9. K_{SOC} effect on battery and gas engine-generator operation.

3.1.4 Influence of K_{GE}

Much like a proportional feedback control returns the battery to a reference state of charge, the gas engine-generator has a similar proportional feedback control returns the gas engine-generator to the nominal output power. The range of the feedback gain (K_{GE}) was selected to be 5%, 10%, 20%, and 50% of the gas engine-generator ramping capability, GE_{RRSat} or 0.285 kW/sec. K_{GE} was selected to be less than GE_{RRSat} in order to prioritize smoothing. Larger K_{GE} values force the GE back toward nominal ($P_{GE} = 0$ kW) quicker, as shown in Figure 10. Since the value of GE_{RRSat} is relatively small, the GE return signal is small, even for the $0.5 \cdot GE_{RRSat}$ case.

Therefore, as will be shown later, the K_{GE} value has little influence on the GE or battery output in the timeframe of interest for smoothing (minutes).

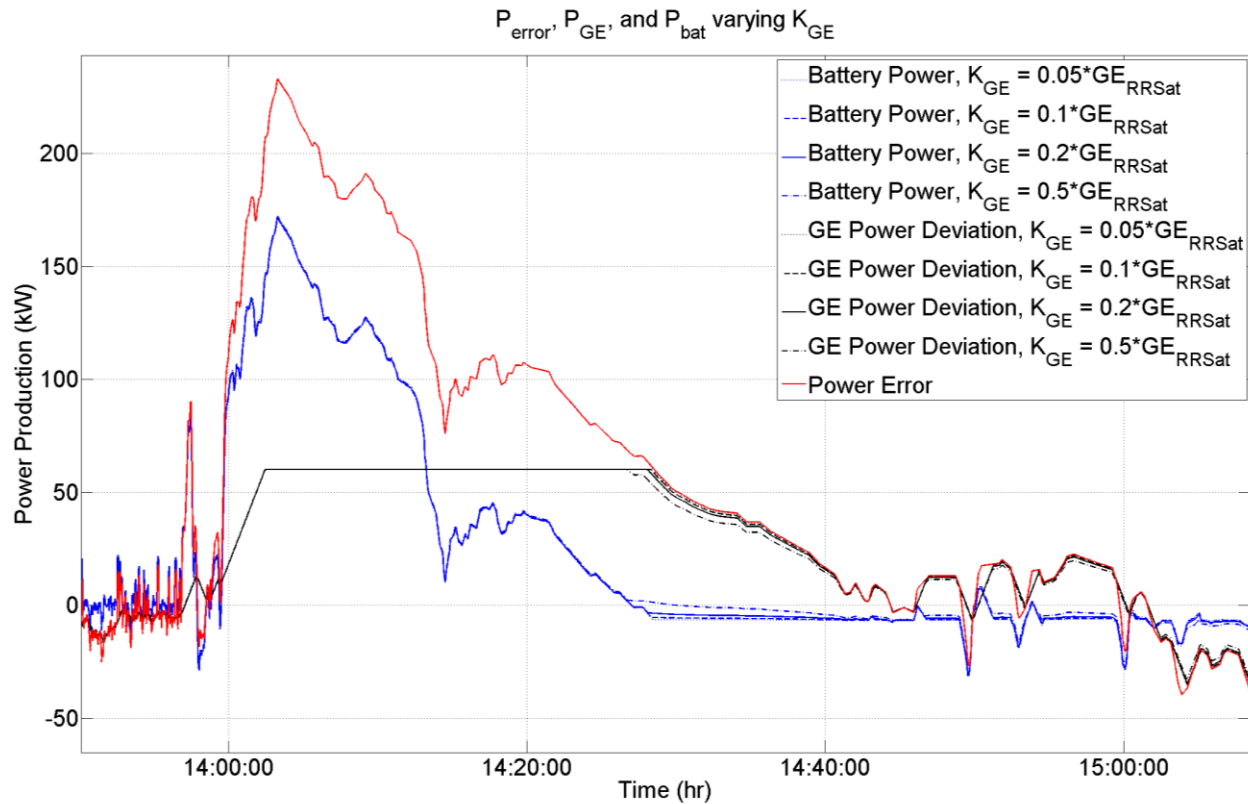


Figure 10. K_{GE} effect on battery and gas engine-generator operation.

3.1.5 Influence of GE Delay

There is a delay in the gas engine-generator power output due to communication lag from the prosperity site to the NEDO plant, as well as control and engine response delays. This has not been determined experimentally. Several scenarios were simulated to determine the impact that delays have on the performance of the smoothing control. As shown in Figure 11, since the GE is relatively slow already—compared to the PV and battery power—there is little influence on the total power production from the smoothing sources (P_{bat} and P_{GE}) with the GE delay. Under these tests, the battery assumes that the GE responds instantly, so there is no change in the P_{bat} due to different GE delays.

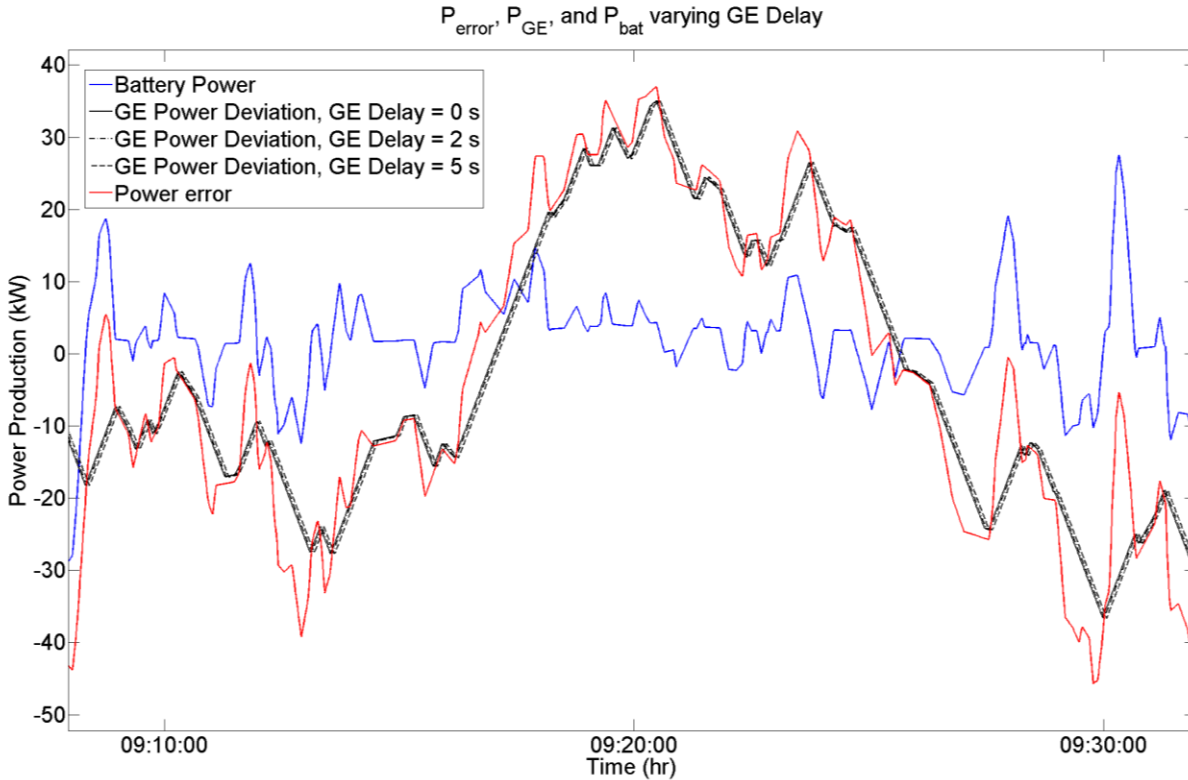


Figure 11. Influence of GE Delay on gas engine-generator operation.

3.2 Figures of Merit

In order to optimize the control parameters, a number of figures of merit (FOMs) were defined to represent different performance metrics and costs. For instance, a system designer may be interested in balancing the cycle life expectancy and size of the battery with the degree of PV smoothing and natural gas engine-generator usage. The FOMs used to represent various performance aspects of the design are as follows:

- **RR₉₉**: The 99th percentile of the 1-minute ramp rate in kW/min for a given test period (e.g., one day with a high degree of PV output variability). (See [13] for details.) This is a good approximation of the degree of smoothing that the control system achieves.
- **BatSOCRange**: The range of battery capacity expressed as the difference between the minimum and the maximum SOC during the simulation. This is used to determine the required capacity of the battery.
- **MaxBatkW**: The maximum output power of the battery during the simulation. This defines the size of the PCS connected to the battery.
- **BatWork**: Total work done by the battery during the simulation in GJ as defined by: $\int |P_{Bat}| dt$. This represents the amp-hour throughput of the battery and is one metric for predicting the lifetime of the battery [14].

- **AvgGEPower**: The average gas engine-generator power production in kW (referenced from nominal). This is a rough estimate—ignoring GE efficiencies—of additional fuel the GE uses compared to running at a nominal 180 kW level.
- **GEwear** = The amount of GE adjustment during the simulation, $\int |P_{GE}| dt$. Larger values indicate the GE power was adjusted more often or by larger amounts. This value is used as a surrogate for wear; although, genset operating time or total kWh could also be used [15].

The simple FOMs described above were developed to illustrate an optimization methodology. They can be further refined or different metrics could be selected that are more suitable for the specific situation.

3.2 Control Optimization

Latin Hypercube Sampling (LHS) was employed to develop an intuitive understanding of the influence of the control parameters on the different figures of merit. The range of the design parameters is shown in Table 1. A total of 500 simulations using different control parameters were conducted for the 5 PV power profiles shown in Figure 12.

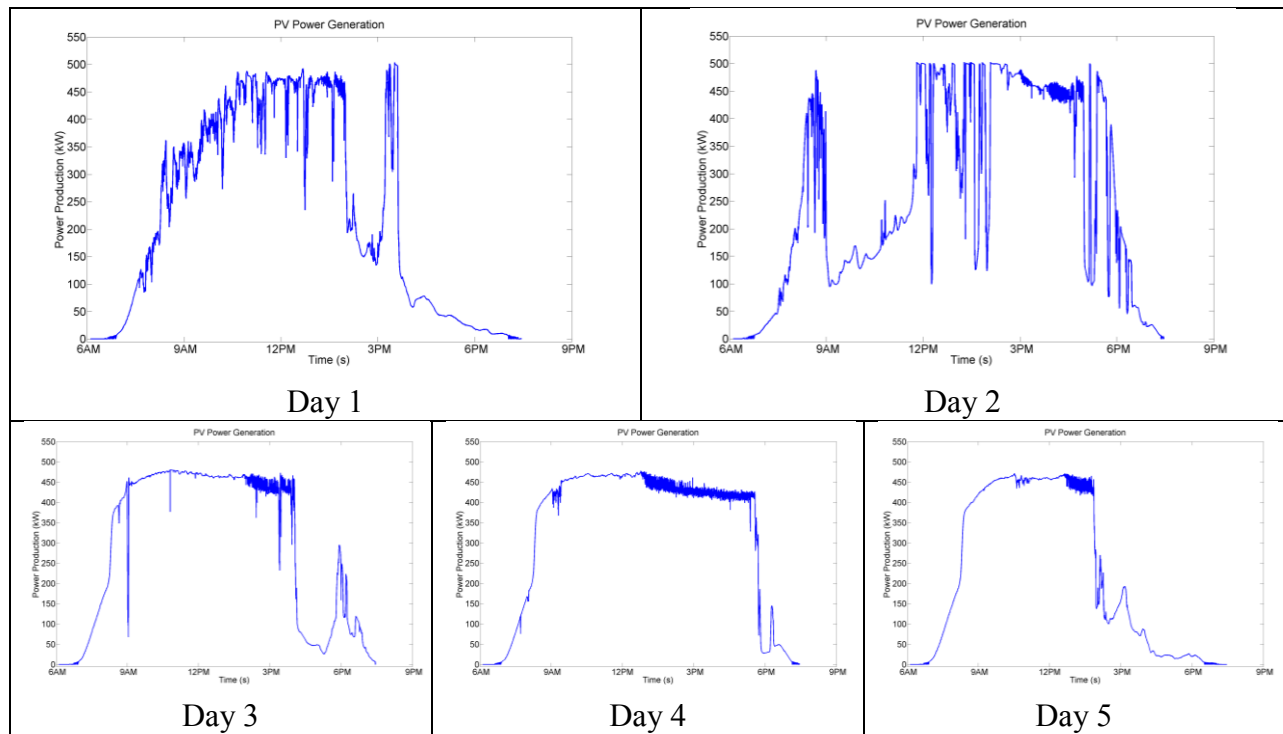


Figure 12. Power profiles for the LHS simulations.

Figure 13 shows the results of the LHS for Day 1. There is substantial information in Figure 13 relating the control parameters to the FOMs. A strong correlation between a parameter and a FOM indicate that parameter has a strong influence on that FOM. The vertical scatter in the plots is the influence of the other parameters on the FOM. Thus, when there is a large vertical scatter, the other parameters play a significant role in that FOM.

Some of the insights that can be gathered from Figure 13 include:

1. When the GE is used, the battery does not work as hard (GEgain vs. BatSOCRange) or need to be as big (GEgain vs. MaxBatkW), and it improves the lifetime of the battery because there are fewer amp-hours cycled through the battery (GEgain vs. BatWork).
2. The GE is not fast enough to help with the highest ramp rates (GEgain vs. RR99).
3. The most critical factor in the ramp rates is the smoothing window size (T_w vs. RR99). For a larger smoothing window the ramp rates drastically decrease.
4. Smoother power means more or larger GE power adjustments (T_w vs. GEwear), and more battery use (T_w vs. BatWork).
5. K_{GE} and GE Delay have little influence on the FOMs based on the correlation values in the last two columns.
6. The rate at which the battery returns to the SOC influences the battery FOMs and the ramp rates. For larger K_{SOC} values, the ramp rates increased slightly (K_{SOC} vs. RR99), the SOC range is reduced slightly (K_{SOC} vs. BatSOCRange), the max battery power output increases (K_{SOC} vs. MaxBatkW), but overall battery use is reduced (K_{SOC} vs. BatWork).
7. Smoother power equates to a need for more battery capacity (T_w vs. BatSOCRange) and larger PCS size (T_w vs. MaxBatkW).
8. There are nonlinearities for some parameters (GEgain vs. MaxBatkW) possibly due to the PV profile for this particular day.
9. The GE works harder when it is GE responding more aggressively to the P_{error} signal (GEgain vs. GEwear).
10. Less genset power is required when the GE is used for smoothing compared to running at nominal power (GEgain vs. AvgGepower), possibly because $\int P_{error} dt$ is negative so there is more need to reduce power than increase power for this day and/or the GE follows the error signal better in morning when it is less cloudy (lower ramp rates) and $P_{error} < 0$.
11. K_{SOC} , K_{GE} and GE Delay have very little impact on the FOMs defined for this example.

Similar conclusions can be made for the other four days.

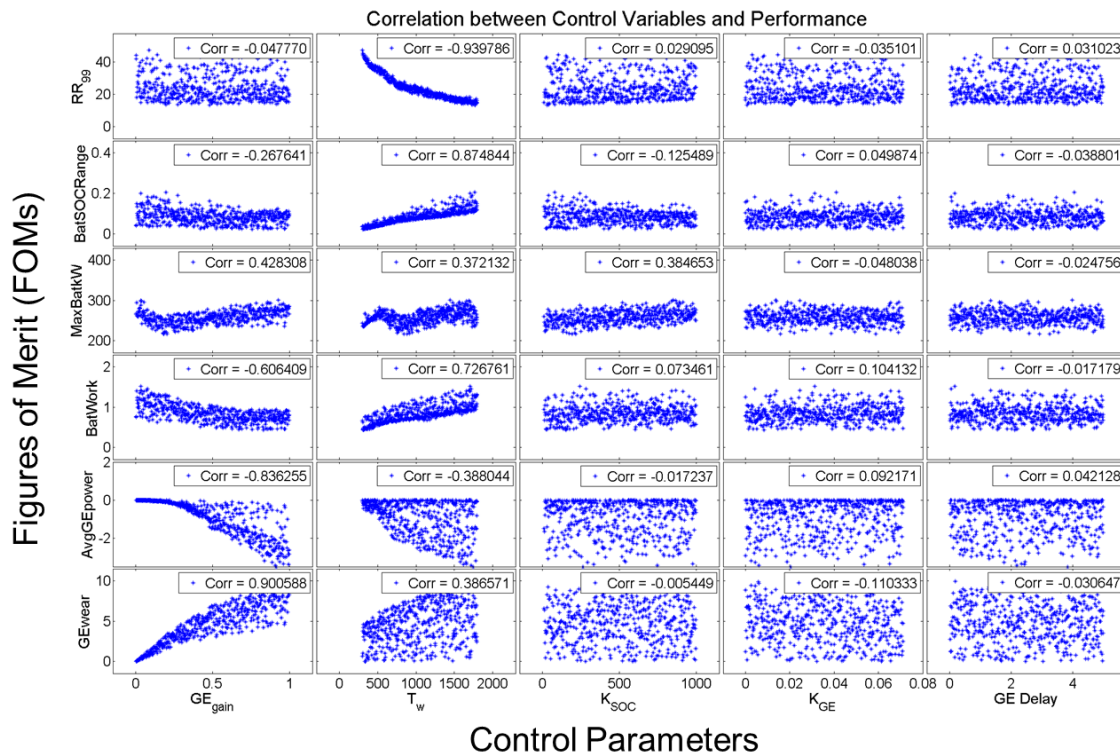


Figure 13. Latin Hypercube Sampling results for Day 1.

Figure 14 compares the results of the LHS for all five days. The figure clearly shows that some of the FOMs are heavily influenced by the PV power output profile. When there is stratification in the LHS matrix it indicates that those FOMs are driven by the PV power profile and not completely by the controller. For instance, the largest ramp rates can be mitigated with larger T_w values, but days with more clouds tend to produce larger ramp rates for smaller T_w values. Similarly, the maximum instantaneous battery output and total work is closely correlated to the days with larger ramp rates. These results also confirm that K_{SOC} , K_{GE} and GE Delay have very little effect on the FOMs.

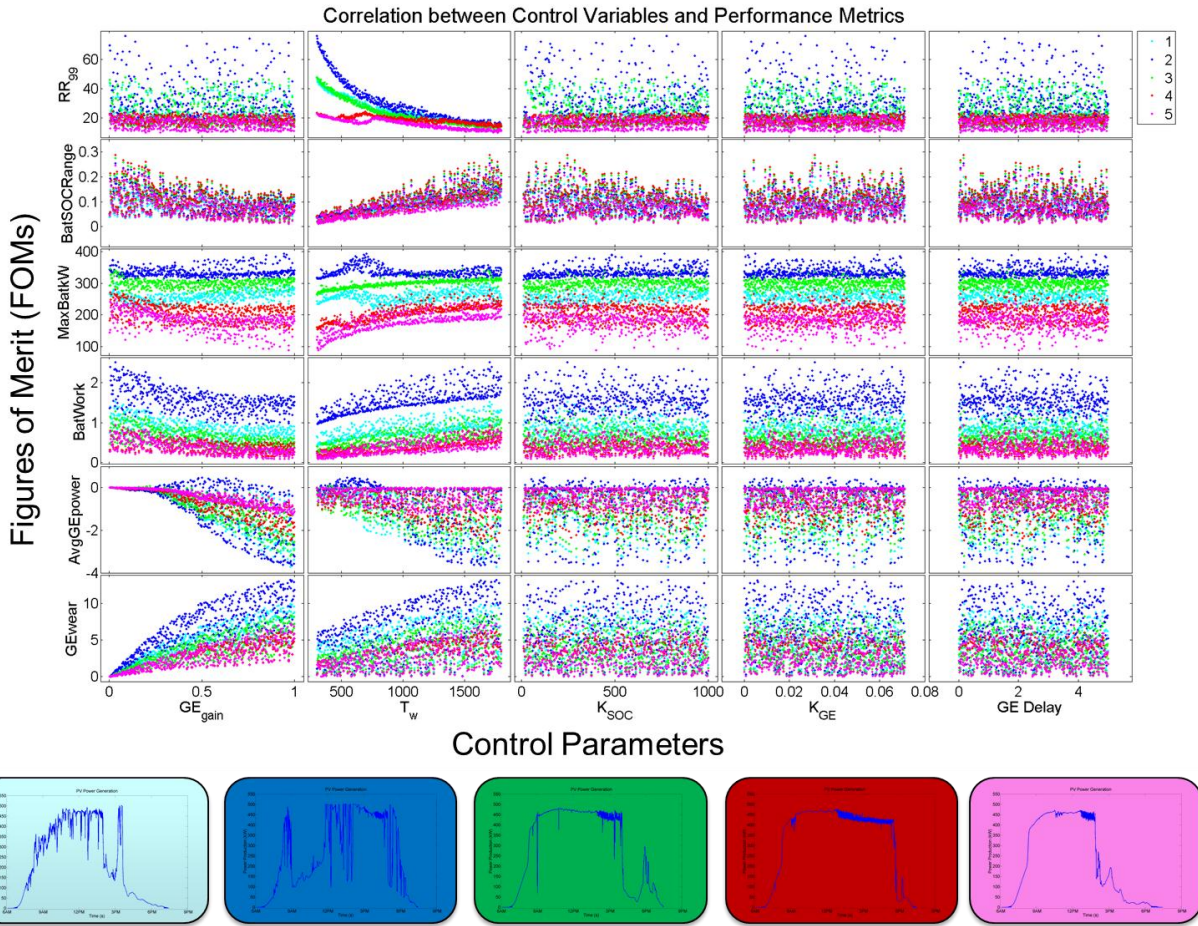


Figure 14. Latin Hypercube results for all 5 days.

To determine the optimal control for the Mesa del Sol system, a cost function based on weighted FOMs factors with additional constraints on FOMs was used. The function and constraints will vary with hardware, climate, and objectives of the owner. For instance, it may be necessary to reduce the ramp rates to a specific level, but this will cycle the battery more and reduce the expected battery cycle life. If larger PV output ramps are acceptable, the battery life could be extended.

As an example, consider a situation where energy storage system is being considered to limit PV ramps to 50 kW/min for a given PV output profile. In this case, there is also an interest in minimizing the battery size while still having a reasonable battery cycle life expectancy. Let's assume that a genset with the characteristics discussed in Section 1 is available, and the control scheme described in Figure 2 is employed. The control fitness function for simulation, i , is,

$$F_i = K_{RR,i} \cdot [f(BatSOCRange_i) + f(BatWork_i)] \quad (2)$$

where

$$K_{RR,i} = \begin{cases} 1 & \text{if } RR_{99,i} < 50 \text{ kW/min} \\ 0 & \text{if } RR_{99,i} > 50 \text{ kW/min} \end{cases} \quad (3)$$

$$f(\text{BatSOCRange}_i) = w_1 \left(\frac{\max(\text{BatSOCRange}) - \text{BatSOCRange}_i}{\max(\text{BatSOCRange})} \right) \quad (4)$$

$$f(\text{BatWork}_i) = w_2 \left(\frac{\max(\text{BatWork}) - \text{BatWork}_i}{\max(\text{BatWork})} \right) \quad (5)$$

The $\max(\text{BatSOCRange})$ and $\max(\text{BatWork})$ values are the largest outputs from the LHS results and used to normalize $f(\text{BatSOCRange}_i)$ and $f(\text{BatWork}_i)$. The weightings w_1 and w_2 are selected based on the relative importance of minimizing the battery size and increasing battery life. Here, w_1 is selected to be 10 and w_2 is 3. The fitness of a controller is designed to be 0 if the controller is unable to keep system power ramps below the design requirement. If the controller keeps ramp rates below 50 kW/min, then the best F_i value will balance the battery size and lifetime.

It should also be noted that this optimization process can also be performed prior to the construction of the PV system. The PV power output can be predicted using irradiance data collected at the site [16] and the battery and gas engine-generator outputs can be simulated in MATLAB/Simulink, as demonstrated previously.

To make the optimization process simpler, the number of input parameters was reduced to GE_{gain} , T_w , and K_{SOC} , because K_{GE} and GE Delay did not significantly influence RR_{99} , BatSOCRange . To illustrate the fitness profile of different controller options, the LHS data was mapped onto the fitness landscape using a maximum of RR_{99} , BatSOCRange , and BatWork for the 5 days. (The LHS parameter values were the same for each of the simulated days.) The results are shown in Figure 15 and shown in 3D in Figure 16. The maximum LHS fitness was achieved with a controller with $T_w = 454.1$, $GE_{\text{gain}} = 0.826$, and $K_{\text{SOC}} = 120.9$.

Since the fitness profile was reasonably smooth even with the steep drop from $K_{RR,i}$, a sequential quadratic programming (SQP) optimizer was selected to determine the optimal control parameters. The SQP optimizer was wrapped around the Simulink simulation for the 2nd day. The optimal controller was determined to be $T_w = 444.83$, $GE_{\text{gain}} = 0.531$, and $K_{\text{SOC}} = 10.0$. This indicates that the lowest T_w values were not suitable for the controller because the ramp rates are too large, but being close to that threshold is desirable because it minimizes the battery size and battery use. If the 50 kW/min limit was a critical boundary (e.g., there would be a contract violation if it was exceeded), then it would likely be better to find a more robust controller with a larger T_w , so that in the event of high solar variability, the maximum ramps requirement would not be crossed.

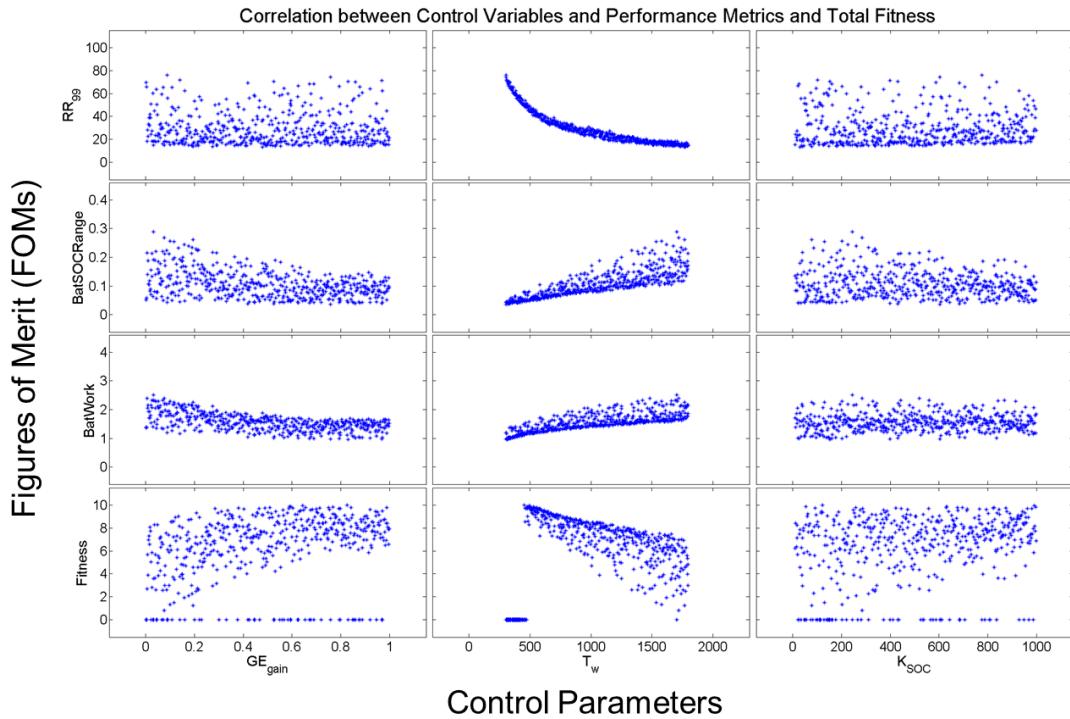


Figure 15. Influence of control parameters on FOMs and total fitness.

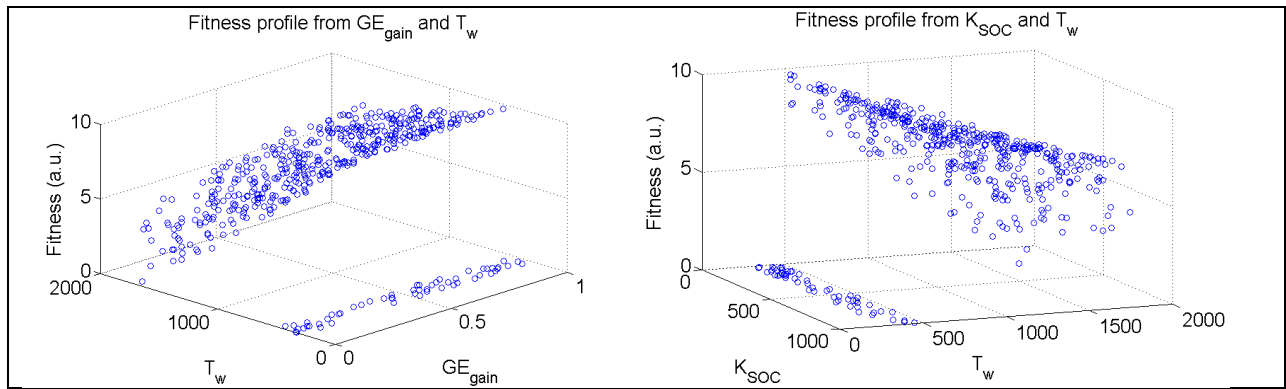


Figure 16. Three-dimensional representation of the fitness profile.

4. Alternative Control Schemes

4.1 Controlling ramp rates with only the battery or gas engine-generator

While in the above simulations there were cooperative PV output smoothing with a gas engine-generator and battery, it is possible that due to maintenance or fault conditions, only one of these systems would be functioning to smooth the PV power. For the specific conditions of the Prosperity project, the battery can provide more power to the grid—and can do so quicker than

the gas engine-generator. Since the PV power output ramping far exceeds the capability of the genset, the genset is unable to reduce large short-term ramps when the battery is unavailable. This effect is shown in Figure 17. The slow response of the GE is reflected in ramp statistics as well, shown in Figure 18. Therefore, when using the same hardware and control architectures, the degree of smoothing provided by the battery alone is nearly equivalent to the battery and the genset as long as the battery does not saturate. The benefit to the coordinated control system is that the GE reduces the battery SOC range, PCS peak power output, and, therefore, increases battery life.

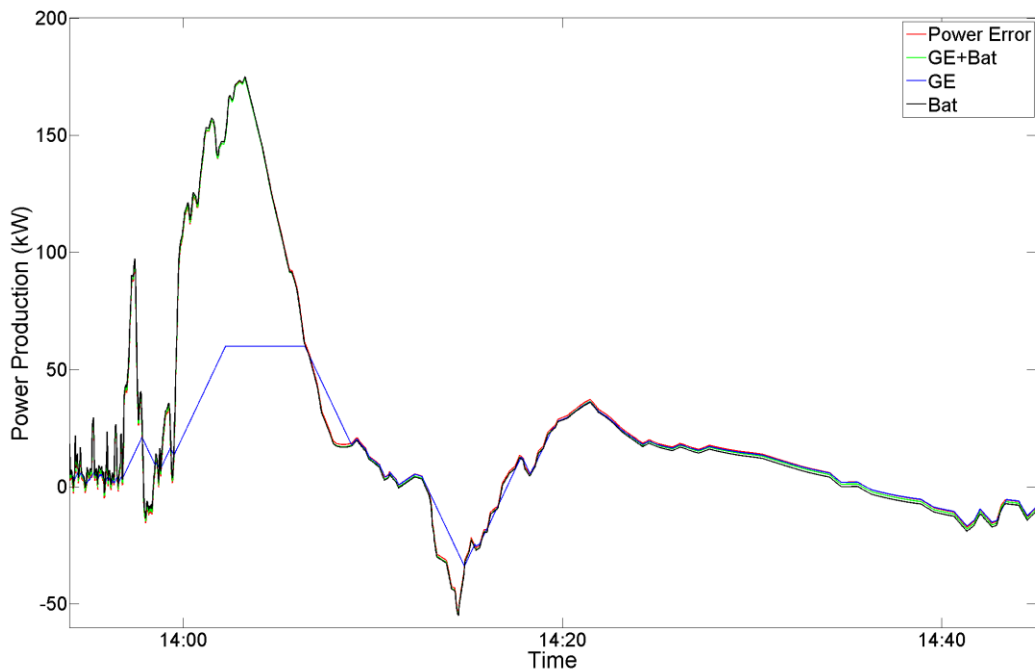


Figure 17. Power production when the GE or battery are unavailable.

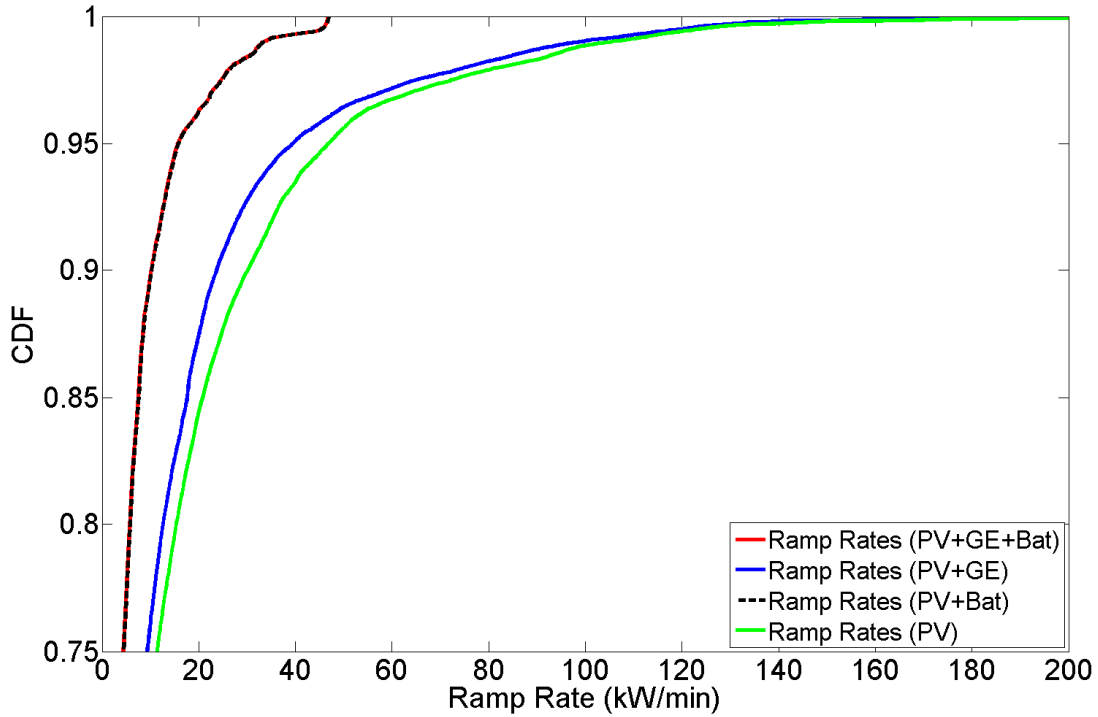


Figure 18. Ramp rate CDFs for Day 1 when the GE or battery are unavailable.

4.2 Simulations without GE-Battery Coordinated Control

A number of studies were performed to determine how smoothing control can be accomplished without coordinated control between the gas engine-generator and battery. In the previous studies, the gas engine-generator output was sent to the battery to update the P_{error} signal; thereby, the slower gas engine-generator simply contributed to the best of its ability, considering ramping limitations, and the battery made up the difference. Here, we consider a situation where the battery operates independent of the GE entirely, as shown in Figure 19. Both the battery and the genset react to the same P_{PV} signal. P_{error} is the same in the GE and battery controls because T_w is the same at both locations. Without the communications link between the GE and battery, $P_{\text{GE}} + P_{\text{bat}} \neq P_{\text{error}}$, but the smoothed output is still significantly better than P_{PV} alone.

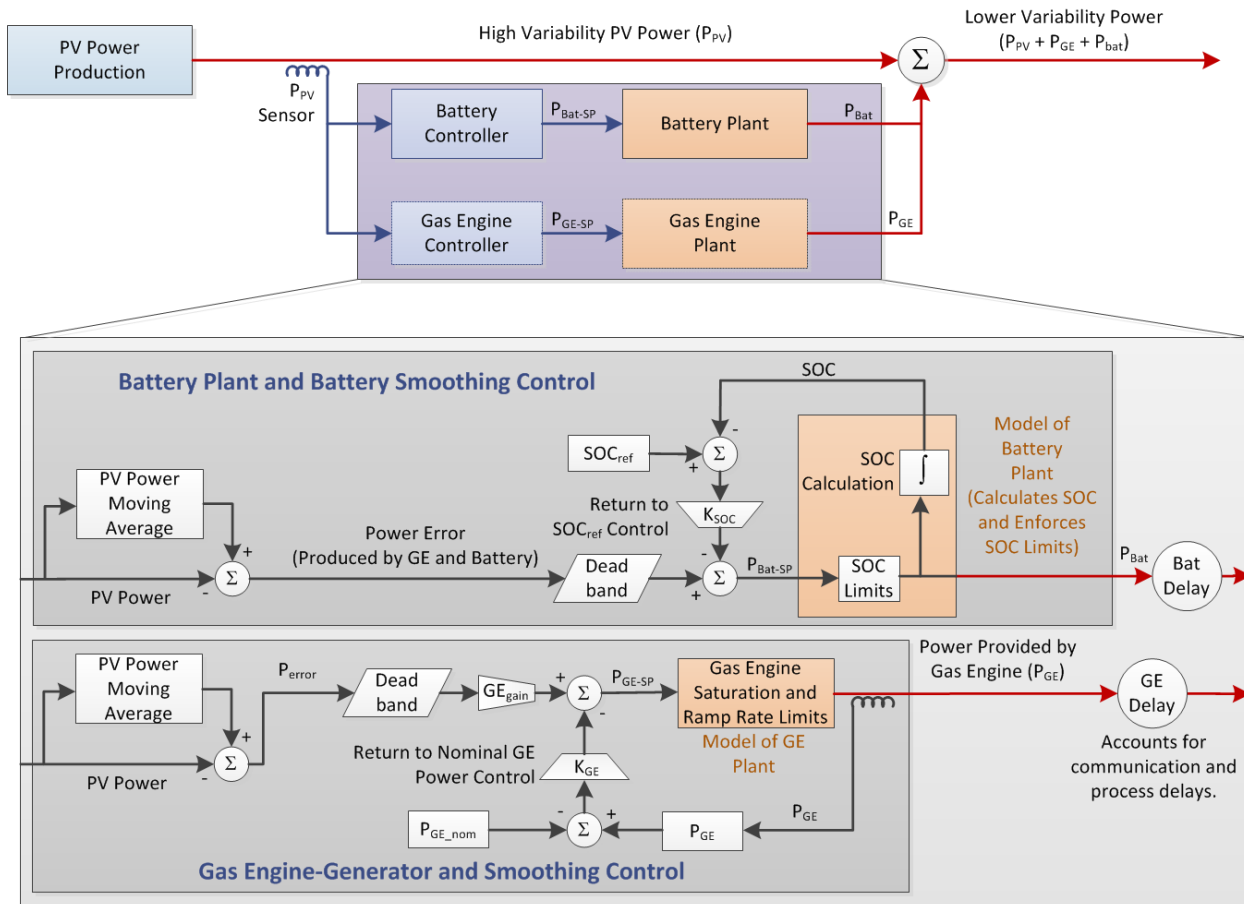


Figure 19. Control scheme for the battery and gas engine-generator without communication from the gas engine-generator to the battery.

In practice, this control architecture results in poorer performance compared to the architecture shown in Figure 2. Without the communication link in the coordinated control case, the battery operates oblivious to the actions taken by the GE, but this is not necessarily a bad thing, as overshooting P_{error} with $P_{\text{GE}} + P_{\text{bat}}$ at times of high ramp rates will still reduce ramps to a reasonable level. In fact, regardless of the communication link between the GE and the battery, the battery does most of the work for the high ramp rate cases, and, therefore, either controller will help with the ramp rates at the 99th percentile of the CDF, shown in Figure 20. The coordinated algorithm typically does a better job balancing ramp rates while minimizing the battery use, but both controllers limit the ramp rates of the system.

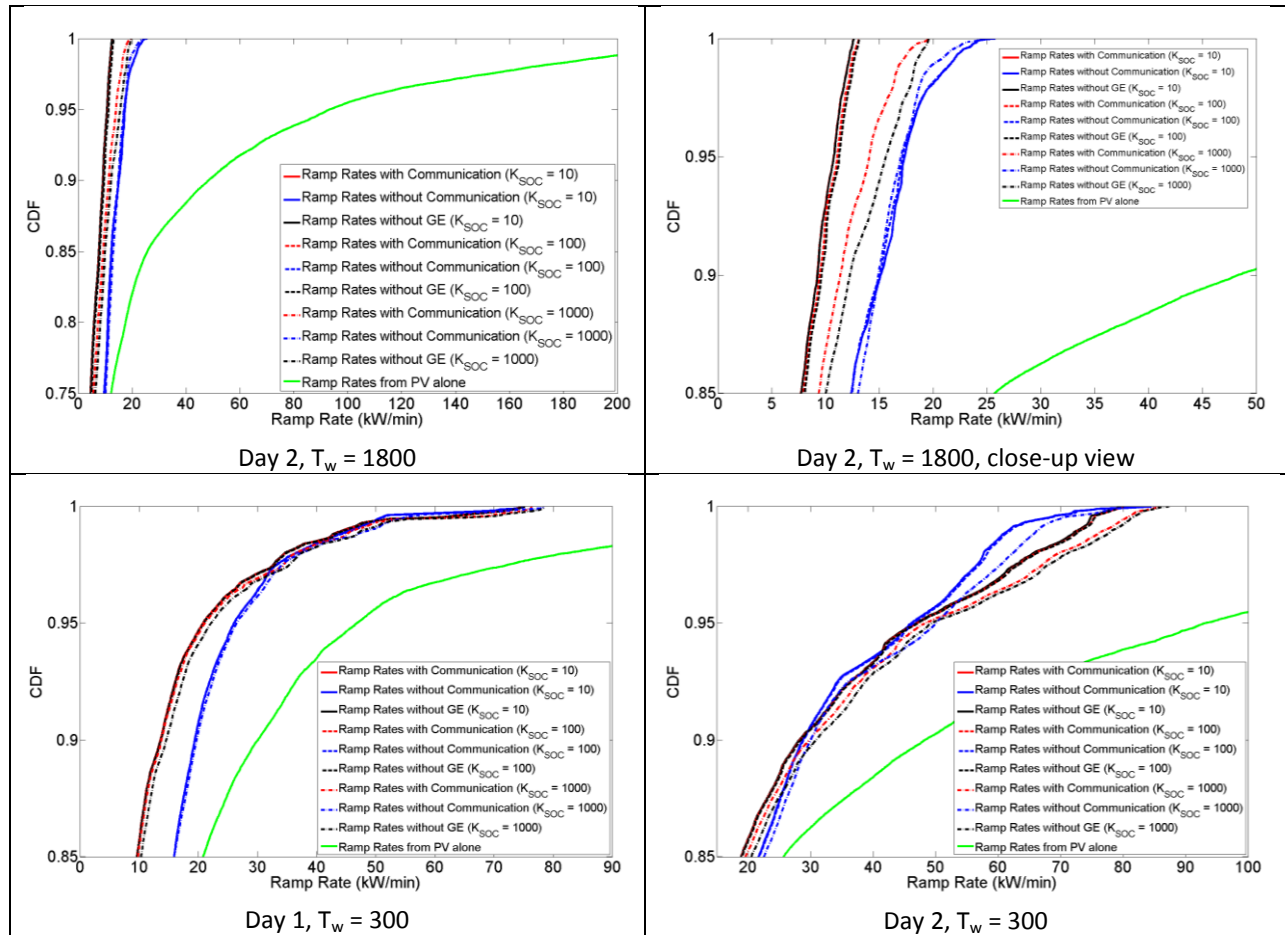


Figure 20. PV smoothing with and without communication from the GE to battery.

To better determine the influence of the communication link on the figures of merit, the LHS samples from Day 2 were simulated with and without coordinated control, shown in Figure 21. The red and blue data points have the same set of control parameter inputs, so there is no influence of LHS randomization. It can be seen that the control coordination has no influence on the gas engine-generator parameters because it operates the same in both simulations. The 99th percentile of ramps, battery SOC range, battery max power output, and battery work are all slightly reduced with control coordination. The largest downside to the uncoordinated control is that the battery and PCS work harder than they need to (MaxBatkW and BatWork), because the GE is making up for some of the P_{error} , but the battery is not aware of it. In either control strategy, note that specific FOM targets can be achieved.

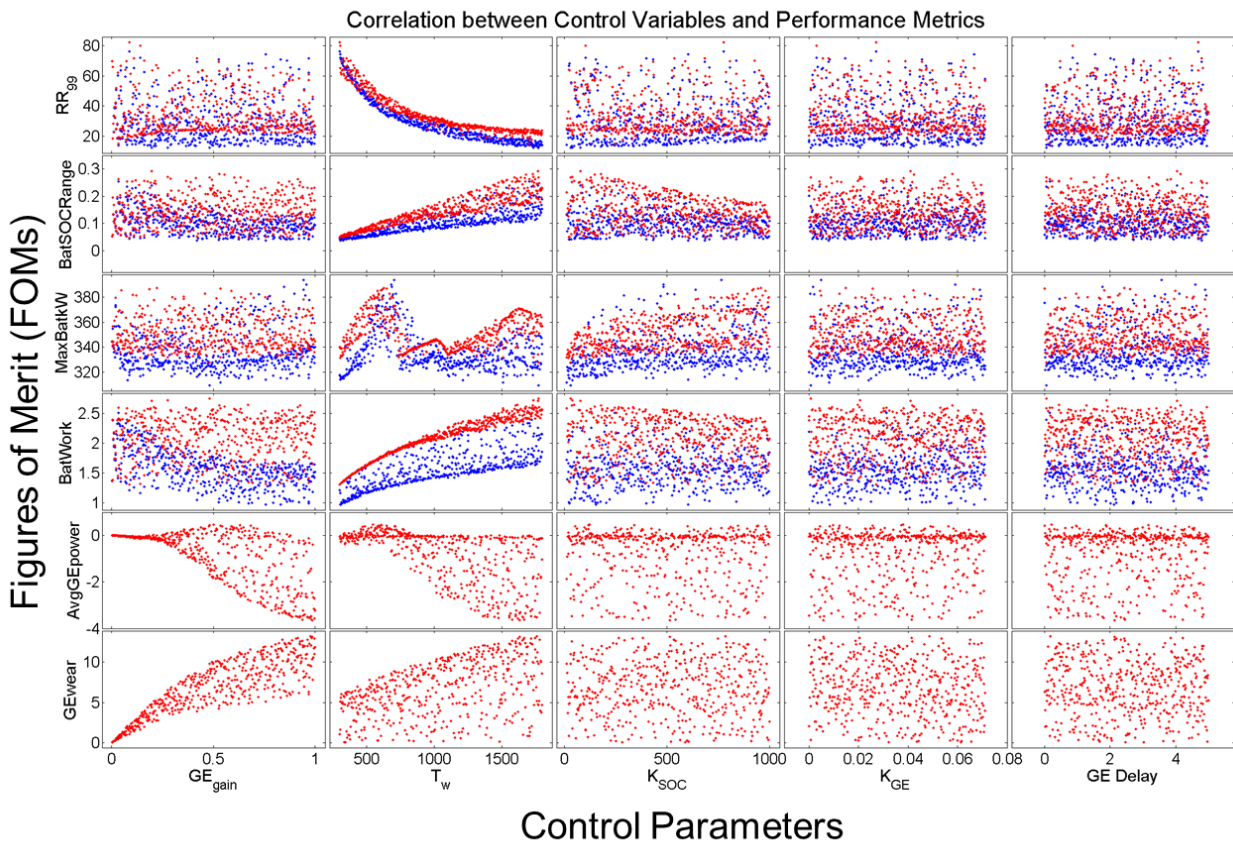


Figure 21: Difference in FOMs depending on communication from the GE to the Battery. Blue is with coordinated control.

5. CONCLUSIONS

Simulations of PV power smoothing control strategies at Mesa Del Sol were performed in MATLAB/Simulink to demonstrate the influence of different control parameters on figures of merit. The controller utilizes both a traditional natural gas genset and a battery to perform the smoothing. The smooth target is calculated using a sliding window on the time history of the PV plant output. Using the gas engine-generator in addition to just a battery for PV power smoothing provides a number of benefits including longer battery life, smaller power conditioning system, and smaller battery capacity.

The simulations show that certain targets (e.g. specific ramp rates) can be reached and the entire system can be optimized by adjusting the control parameters. Some control parameters were found to influence the figures of merit more than others. Most critical control parameters on the figures of merit were the amount of GE use, battery SOC return signal, and, most importantly, sliding window size. The control parameters could be tuned to minimize battery and GE use or decrease the system ramp rates. These trade-offs were considered to find an optimal control for a theoretical set of constraints and design objectives.

It was determined that if the gas engine-generator was unavailable, there would be little effect on the ramp rates, but the battery SOC range and PCS size would be larger. If the battery was not available the GE would not be able to control the ramp rates well. Finally, the influence of communications between the GE and battery were simulated: without a GE-to-battery communication link, there is a slight reduction in performance of the overall system because the battery is overused.

REFERENCES

- [1] O. Lavrova, F. Cheng, S. Abdollahy, A. Mammoli, S. Willard, B. Arellano, and C. van Zeyl, "Modeling of PV plus Storage for Public Service Company of New Mexico's Prosperity Energy Storage Project," 2011 Electrical Energy Storage Applications & Technologies Conference (EESAT), San Diego, CA, Oct. 16-19, 2011.
- [2] A. Ellis and D. Schoenwald, PV Output Smoothing with Energy Storage, Sandia Technical Report, SAND2012-1772, March 2012.
- [3] S. Abdollahy, A. Mammoli, F. Cheng, A. Ellis, and J. Johnson, Distributed Compensation of a Large Intermittent Energy Resource in a Distribution Feeder, IEEE PES Innovative Smart Grid Technologies (ISGT), 24-27 Feb., 2013.
- [4] T. Hund, S. Gonzalez, and K. Barrett, "Grid-Tied PV System Energy Smoothing," 35th IEEE Photovoltaics Specialists Conference (PVSC), Honolulu, HI, pp. 2762-2766, June 20-25, 2010.
- [5] H. Fakham, D. Lu, and B. Francois, "Power Control Design of a Battery Charger in a Hybrid Active PV Generator for Load-Following Applications," IEEE Transactions on Industrial Electronics, Vol. 58, No. 1, pp. 85-94, Jan. 2011.
- [6] M. Khalid, A.V. Savkin, A model predictive control approach to the problem of wind power smoothing with controlled battery storage, Renewable Energy, vol. 35, no. 7, pp. 1520-1526, July 2010.
- [7] S. Teleke, M.E. Baran, S. Bhattacharya, A.Q. Huang, "Optimal Control of Battery Energy Storage for Wind Farm Dispatching," *IEEE Transactions on Energy Conversion*, vol. 25, no. 3, pp. 787-794, Sept. 2010.
- [8] KEMA, Inc., Lanai PV Interconnect Requirements Study: System Impact Study, June 5, 2008, Interconnection Customer: SunPower, KEMA, Inc., Raleigh, NC, USA, 26707.
- [9] Puerto Rico Electric Power Authority, Minimum Technical Requirements for Interconnection of Photovoltaic Facilities, 2012.
- [10] M. Coddington and A. Ellis, Updating Interconnection Screens for PV Integration Con Streamline Deployment, Solar Industry, Vol. 5, No. 8. pp. 70-74, Sept. 2012.
- [11] P Denholm, E. Ela, B. Kirby, and M. Milligan, The Role of Energy Storage with Renewable Electricity Generation, NREL Technical Report, NREL/TP-6A2-47187, January 2010.
- [12] C. Lenox, PV and Energy Storage: Beyond the Hype, Solar Power International, 12 Sept. 2012.

- [13] J. Johnson, B. Schenkman, A. Ellis, J. Quiroz, and C. Lenox, "Initial Operating Experience of the 1.2-MW La Ola Photovoltaic System," 38th IEEE PVSC, Austin, TX, 4 June, 2012.
- [14] H. Bindner, T. Cronin, P. Lundsager, J.F. Manwell, U. Abdulwahid, and I. Baring-Gould, Lifetime modelling of lead acid batteries. Risø-R Report, Risø-R-1515(EN), 2005.
- [15] M. Muselli, G. Notton, A. Louche, Design of hybrid-photovoltaic power generator, with optimization of energy management, Solar Energy, vol. 65, no. 3, pp 143-157, 1 Feb. 1999.
- [16] C.W. Hansen, J.S. Stein, and A. Ellis, *Simulation of 1-Minute Power Output from Utility-Scale Photovoltaic Generation Systems*, SAND2011-5529, Sandia National Laboratories, Albuquerque, NM, 2011.

DISTRIBUTION

1	MS0352	Jay Johnson	01718
1	MS0352	W. Kent Schubert	01718
3	MS1033	Abraham Ellis	06112
1	MS1033	Charles J. Hanley	06112
1	MS1108	Dan Borneo	06111
1	MS1108	Ross Guttromson	06113
1	MS1108	Benjamin L. Schenkman	06113
1	MS1140	David A. Schoenwald	06113
1	MS0899	Technical Library	09532 (<i>electronic copy</i>)



Sandia National Laboratories